Cell Death and Differentiation (2007) 14, 230–239

www.nature.com/cdd

ER stress (PERK/eIF2α phosphorylation) mediates the polyglutamine-induced LC3 conversion, an essential step for autophagy formation

Y Kouroku[1], E Fujita[1], I Tanida[2], T Ueno[2], A Isoai[3], H Kumagai[3], S Ogawa[4], RJ Kaufman[5], E Kominami[2] and T Momoi*[,1]

Expanded polyglutamine 72 repeat (polyQ72) aggregates induce endoplasmic reticulum (ER) stress-mediated cell death with caspase-12 activation and vesicular formation (autophagy). We examined this relationship and the molecular mechanism of autophagy formation. Rapamycin, a stimulator of autophagy, inhibited the polyQ72-induced cell death with caspase-12 activation. PolyQ72, but not polyQ11, stimulated Atg5-Atg12-Atg16 complex-dependent microtubule-associated protein 1 (MAP1) light chain 3 (LC3) conversion from LC3-I to -II, which plays a key role in autophagy. The eucaryotic translation initiation factor 2 α (eIF2α) A/A mutation, a knock-in to replace a phosphorylatable Ser[51] with Ala[51], and dominant-negative PERK inhibited polyQ72-induced LC3 conversion. PolyQ72 as well as ER stress stimulators upregulated Atg12 mRNA and proteins via eIF2α phosphorylation. Furthermore, *Atg5* deficiency as well as the eIF2α A/A mutation increased the number of cells showing polyQ72 aggregates and polyQ72-induced caspase-12 activation. Thus, autophagy formation is a cellular defense mechanism against polyQ72-induced ER-stress-mediated cell death by degrading polyQ72 aggregates, with PERK/eIF2α phosphorylation being involved in polyQ72-induced LC3 conversion.
Cell Death and Differentiation (2007) **14,** 230–239. doi:10.1038/sj.cdd.4401984; published online 23 June 2006

An autophagic pathway is a cellular defense process involving the bulk degradation of cellular contents by autophagosomes/lysosomes during starvation or viral infection.[1] However, over production of autophagic vesicles interferes with normal membrane trafficking in the cell and causes autophagic cell death with the degradation of cellular organs. These autophagic vesicles are also shown during neurodegeneration such as Huntington disease (HD) with expanded polyglutamine (polyQ) aggregation and Parkinson's disease with α-synuclein aggregation.[2,3]

The molecular mechanism of autophagy has been investigated in yeast and mammalian cells.[4,5] The Atg5-dependent conversion of microtubule-associated protein 1 (MAP1) light chain 3 (LC3), the mammalian homolog of *Atg8*, from LC3-I (free form) to LC3-II (membrane-bound form) is a key step in the induction of autophagy in mammalian cells.[5,6] ProLC3 is processed to LC3-I by cleavage at the C-terminal region[7] immediately after synthesis, and then LC3-I is targeted to the isolated membrane (LC3-II), dependent on the Atg5–Atg12 complex throughout the course of membrane elongation.[5,8] Atg16 homo-oligomers crosslink multiple Atg5–Atg12 conjugates to form Atg5–Atg12–Atg16 complex.[9] During these processes, LC3-I and Atg12 are activated by Atg7.

Recently, an *Atg7*-deficient mouse model showed the accumulation of ubiquitinated proteins and abnormal cellular organs in the liver.[10] These results strongly suggest that autophagy as well as the ubiquitin/proteasome system is involved in protein degradation in addition to the degradation of cellular organs. Rapamycin (Rap), which stimulates autophagy,[11] attenuates polyQ aggregate formation and decreases polyQ toxicity in cell and mouse models of HD.[12,13] This suggests that autophagy seems to contribute to the cellular defense system, by degrading malfolded protein aggregates, as well as cellular dysfunction. However, little is known about the activation of the autophagic pathway in cells expressing malfolded protein aggregates.

The relationship between the intracellular aggregation of malfolded proteins and endoplasmic reticulum (ER) stress has been intensively examined.[14] Excess amounts of unfolded or malfolded proteins in the ER are retrotranslocated to the cytoplasm and degraded by the ER-associated ubiquitine/proteasome degradation (ERAD) system.[15] However, if the amount of unfolded and malfolded proteins exceeds the capacity of the ERAD system, the proteins start to aggregate in the ER and trigger ER-stress-mediated cell death with caspase-12 activation, a caspase specifically

[1]Divisions of Development and Differentiation, National Institute of Neuroscience, 4-1-1 Ogawahigashi-machi, Kodaira, Tokyo 187-8502, Japan; [2]Department of Biochemistry, Juntendo University School of Medicine, 2-1-1, Hongo, Bunkyo-ku, Tokyo 113-8421, Japan; [3]Asahi Glass Co., 1150 Hasawa-cho, Kanagawa-ku, Yokohama, Kanagawa 221-0863, Japan; [4]Department of Neuroanatomy, Kanazawa University Medical School, 13-1, Takara-machi, Kanazawa, Ishikawa 920-8640, Japan and [5]Howard Hughes Medical Institute and Department of Biological Chemistry, University of Michigan Medical Center, Ann Arbor, MI 48109-0650, USA
*Corresponding author: T Momoi, Divisions of Development and Differentiation, National Institute of Neuroscience, 4-1-1 Ogawahigashi-machi, Kodaira, Tokyo 187-8502, Japan. Tel: +81-42-341-2711; Fax: +81-42-346-1754; E-mail: momoi@ncnp.go.jp
Keywords: polyglutamine; ER stress; autophagy; eIF2α; caspase-12
Abbreviations: Bre, brefeldin A; CHOP, C/EBP homologous protein; DN, dominant-negative; eIF2α, eucaryotic translation initiation factor 2 α; ER, endoplasmic reticulum; ERAD, ER-associated degradation; EGFP, green fluorescent protein; HBSS, Hank's Balanced Salt Solution; HD, Huntington's disease; LC3, microtubule-associated protein 1 (MAP1) light chain 3; MEF, mouse embryonic fibroblast; mTOR, mammalian target of rapamycin; PKR, protein kinase regulated by RNA; PERK, PKR-like ER kinase; polyQ, polyglutamine; Thap, thapsigargin; Tm, tunicamycin; Rap, rapamycin; 3MA, 3-methyladenine
Received 01.12.05; revised 13.4.06; accepted 03.5.06; Edited by M Piacentini; published online 23.6.06

localized at ER.[16,17] The cytoplasmic aggregates of malfolded proteins such as polyQ also stimulate ER stress signals and induce ER-stress-mediated cell death with caspase-12 activation in mouse cells, presumably by the accumulation of unfolded proteins in the ER due to the inhibition of ERAD and retrotranslocation.[18,19]

Here, we show that Rap inhibits the polyQ-induced ER-stress-mediated cell death with caspase-12 activation. These results strongly suggest the close relationship between autophagy formation and ER stress signals in cells expressing cytoplasmic polyQ aggregates. In the present study, we used the expanded polyglutamine 72 repeat (polyQ72) and examined the relationship between degradation of intracellular aggregation of malfolded proteins by autophagy and ER stress signals.

Results

Rap inhibits polyQ-induced ER-stress-mediated cell death. PolyQ72 forms cytoplasmic aggregates in C2C5 cells 48 h after transfection of pEGFP (green fluorescent protein)-72CAG and induces ER-stress-mediated cell death with caspase-12 activation during aggregation, while polyQ11 does not form aggregates nor induce the caspase-12 activation.[18] To clarify the relation between autophagy and ER-stress-mediated cell death in cells showing polyQ72 aggregates, we examined the effect of Rap, a stimulator of autophagy, and 3-methyladenine (3MA), an inhibitor of autophagy, on polyQ72-induced caspase-12 activation and DNA fragmentation. Rap decreased the amount of insoluble polyQ72 and inhibited caspase-12 activation, about 50% decrease of the amount of the active form fragment, and DNA fragmentation, whereas 3MA increased the amount of insoluble polyQ72 and stimulated caspase-12 activation, about 2.0-fold increase of the amount of the active form fragment, and DNA fragmentation (Figure 1a).

Rap decreased the number of cells showing polyQ72 aggregates, antiactivated caspase-12 (anti-m12D341) immunoreactivity, and apoptotic feature in cells expressing polyQ72, whereas 3MA increased their cell numbers (Figure 1b and c). However, 3MA did not stimulate polyQ11 aggregation and did not induce caspase-12 activation and DNA fragmentation in cells expressing polyQ11 (Figure 1a–c). These results suggest that autophagy formation is involved in the inhibition of ER-stress-mediated cell death by degrading polyQ72 aggregates.

PolyQ-induced Atg5-dependent LC3 conversion. PolyQ72 induced the conversion of LC3-I (18 kDa) to -II (16 kDa), a key molecule involved in autophagosome formation, in C2C5 cells, but polyQ11 did not (Figure 2a). Deficiency of *Atg5*, a key molecule in the conversion of LC3-I to -II, inhibited the polyQ72-induced LC3 conversion (Figure 2b). During autophagosome formation, LC3-I was converted to LC3-II, which is tightly associated with the autophagosomal membrane. LC3-I is diffusely stained by anti-LC3 in the cytoplasm of cells with no stress, while LC3-II shows bright vesicular and granular anti-LC3 immunostaining with increased fluorescence intensity.[7,20,21] Anti-LC3-positive granules

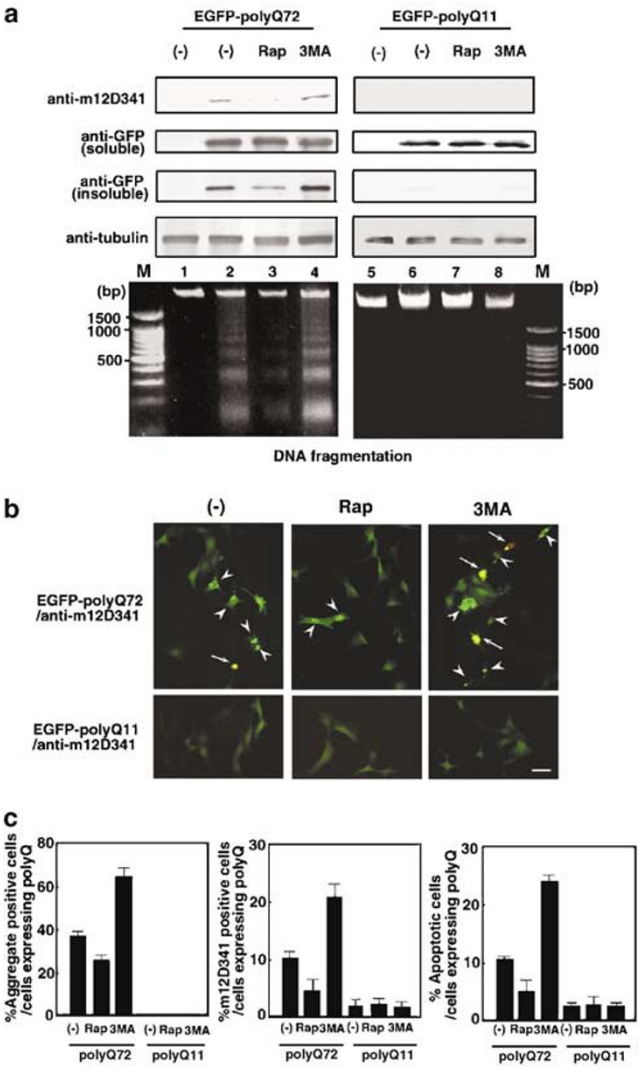

Figure 1 Effect of Rap and 3MA on polyQ11 and polyQ72 aggregation and polyQ aggregate-induced ER-stress-mediated cell death. (**a**) Effect of Rap and 3MA on polyQ11 and polyQ72 aggregate-induced caspase-12 activation and DNA fragmentation. C2C5 cells were transfected with pEGFP-11CAG or pEGFP-72CAG and incubated in the presence or absence of Rap (10 μg/ml) or 3MA (10 mM), and the caspase-12 activation and cell death were examined by immunoblot analysis or DNA fragmentation. lanes 1, 5; untreated cells, lanes 2, 6; polyQ72 or polyQ11 transfected cells, respectively, lanes 3, 7; Rap treated with polyQ72 or polyQ11 transfected cells, respectively, lanes 4, 8; 3MA treated with polyQ72 or polyQ11 transfected cells, respectively. M, DNA size makers. (**b**) Immunofluorescence images of polyQ11 or polyQ72 aggregation (green) and caspase-12 activation (red) in the presence or absence of Rap or 3MA. Arrowheads indicate polyQ72 aggregates and arrows indicate the cells colocalizing caspase-12 activation and polyQ72 aggregates. Scale bar, 25 μm. (**c**) Effects of Rap and 3MA on polyQ11 and polyQ72 aggregation, polyQ11- and polyQ72-induced caspase-12 activation, and polyQ11- and polyQ72-induced cell death. Percentages of cells showing polyQ aggregates, caspase-12 activation, or apoptotic feature in cells expressing polyQ11 or polyQ72 were determined in the presence or absence of Rap or 3MA as described in Materials and Methods. Error bars represent S.E.M. of the percentage of cells with polyQ aggregates (left panel), cells with caspase-12 activation (middle panel) or cells showing apoptotic future (right panel) within cells expressing polyQ

were detected in the cytoplasm of cells showing polyQ72 aggregates but not observed in cells expressing polyQ11 (Figure 2c) and in *Atg5*-deficient mouse embryonic

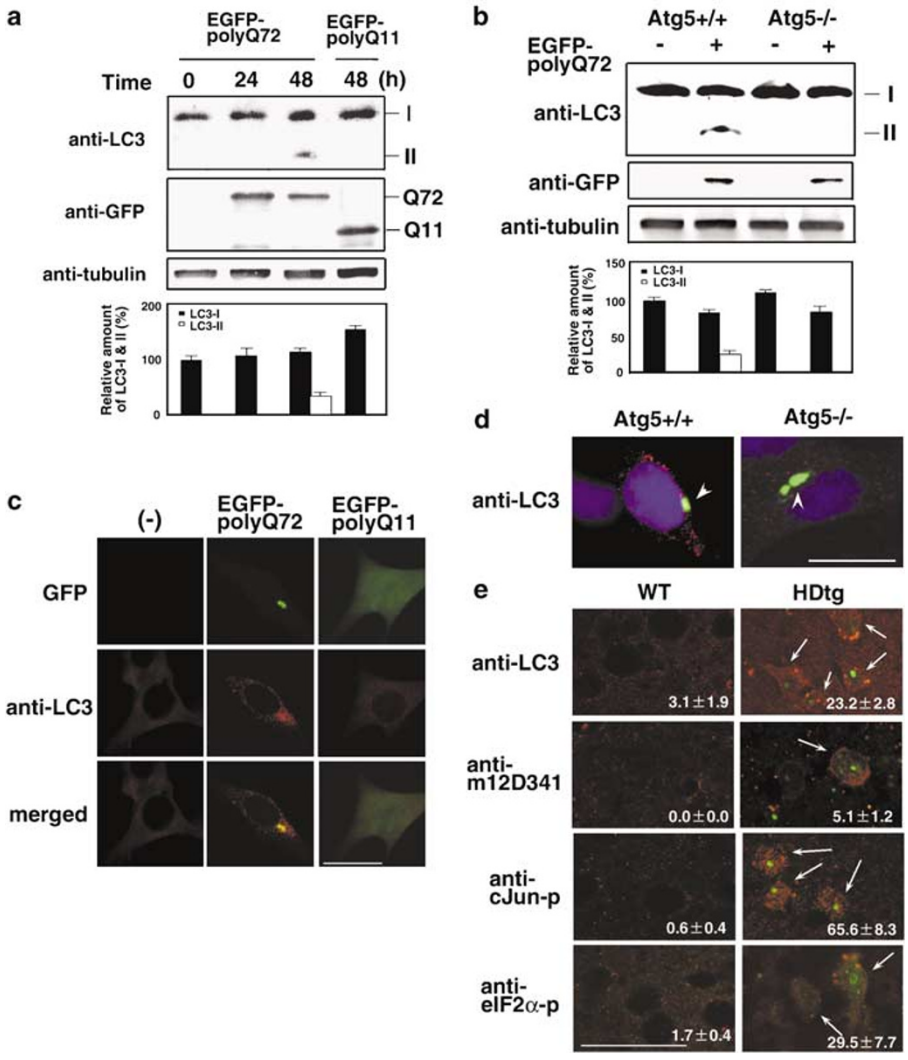

Figure 2 PolyQ72-induced Atg5-dependent LC3 conversion. (**a**) PolyQ-induced conversion of LC3-I to -II. After pEGFP-72CAG or pEGFP-11CAG was transfected into C2C5 cells, the conversion of LC3-I to -II was examined in a time-dependent manner by immunoblot analysis. The lower panel indicates the relative amounts of LC3-I (closed bars) an LC3-II (open bar) showing densitometric analyses. Error bars represent S.E.M. of the LC3-I and -II percentage of density. (**b**) Effect of *Atg5*-deficiency on polyQ72-induced LC3 conversion. After pEGFP-72CAG was transfected into Atg5 $+/+$ and Atg5 $-/-$ MEF cells, the LC3 conversion was examined by immunoblot analysis. The lower panel indicates the relative amounts of LC3-I (closed bars) an LC3-II (open bar) showing densitometric analyses. Error bars represent S.E.M. of the LC3-I and -II percentage of density. (**c**) Effect of polyQ72 aggregates on the LC3 distribution. LC3 distribution in nontransfected cells, cells expressing EGFP-polyQ72, and -polyQ11 were examined. (Upper panels) EGFP-labeled; green, (middle panels) anti-LC3, rhodamine; red, (lower panels) merged images. Anti-LC3 granular immunoreactivity was detected in cells expressing polyQ72 aggregates. The polyQ aggregate colocalized with anti-LC3. (**d**) Effect of *Atg5*-deficiency on the LC3 distribution. Atg5 $+/+$ and Atg5 $-/-$ MEF cells were transfected with pEGFP-72CAG (EGFP-labeled: green), and immunofluorescence images of LC3 distribution was detected by immunostaining using anti-LC3 (rhodamine: red; Hoechst 33342: blue). Arrowheads indicate EGFP-polyQ72 aggregates. In contrast with Atg5 $+/+$ MEF cells, the colocalization is not detected in the ATG5 $-/-$ MEF cells. (**e**) Double immunostaining with anti-LC3, anti-c-Jun-p, anti-eIF2α-p, or anti-m12D341 (rhodamine: red) and anti-huntingtin (EM48) (FITC: green) in the brain tissues from transgenic R6/2 mice, a mouse model of HD. Anti-LC3 granular immunoreactivity and anti-m12D341, anti-c-Jun-p, anti-eIF2α-p immunoreactivity were detected in the HD mouse brain (HDtg) but not in the WT mouse brain. Arrows indicate immunoreactive cells. The numbers indicate the population of immunoreactive cells. Scale bars, 25 μm

fibroblasts (Atg5-/-MEF) cells showing polyQ72 aggregates (Figure 2d). Thus, granular anti-LC3 immunostaining is available for detection of the polyQ72-induced Atg5-dependent LC3 conversion leading to autophagy. ER stress inducers, such as tunicamycin (Tm), brefeldin A (Bre), and thapsigargin (Thap), as well as starvation, also induced LC3 conversion and anti-LC3 granular immunoreactivities (see Supplemental Figure 1a and b).

PolyQ aggregates are also detected in the brain of R6/2 mouse, an HD model mouse expressing a truncated form of huntingtin with polyQ144.[22] We examined the relationship between LC3 conversion and ER stress in the brain of R6/2 mouse by immunostaining (Figure 2e). Anti-LC3 granular immunoreactivity was detected in 23.2 $\pm$ 2.8% of cells expressing polyQ144 aggregates in the brain of R6/2. In addition, caspase-12 activation, a sign of ER stress cell death, was also detected in 5.1 $\pm$ 1.2% cells showing polyQ144 aggregates in the R6/2 mouse brain, but undetectable in the wild-type (WT) mouse brain. Furthermore, c-Jun phosphorylation, and eucaryotic translation initiation factor 2 α (eIF2α)

phosphorylation, responsive signals to ER stress, were positive in 65.6 ± 8.3, and 29.5 ± 7.7% of cells showing polyQ aggregates, respectively.

PolyQ72 aggregates-induced LC3 conversion with lysosomal turnover of LC3-II. A cellular level of LC3-II does not always show the stimulation of LC3 conversion because autophagosomal LC3-II is degraded by lysosomal hydrolases after formation of autolysosomes; the inhibition of the fusion of autophagosome with lysosome as well as the stimulation of LC3 conversion increases the level of LC3-II. LC3-II significantly accumulates in the presence of E64d, a membrane-permeable inhibitor of cathepsins B, H, and L, and pepstatin A, an inhibitor of cathepsins D and E, under starvation conditions.[23] Lysosomal turnover of LC3-II reflects autophagic activity. We examined the effect of E64d and pepstatin A on the level of polyQ72 and the polyQ72-induced LC3-II. The polyQ72, but not polyQ11, accumulated in the insoluble fraction and polyQ72-induced LC3-II also accumulated (Figure 3a). E64d and pepstatin A increased the number of cells showing polyQ72 aggregates, however, did not stimulate polyQ11 aggregation (Figure 3b and c). The increased level of LC3-II induced by polyQ72 was due to the stimulation of the LC3 conversion but not due to the inhibition of the fusion of autophagosome with lysosome. Thus, polyQ72 and polyQ72-induced LC3-II in the autophagosome were degraded in the autolysosome. The cells degradated polyQ72 aggregates in the autolysosome by promoting the LC3 conversion and increasing the autophagic activity.

PolyQ-induced LC3 conversion via PERK/eIF2α-phosphorylation. LC3-I is targeted to the isolated membrane (LC3-II), dependent on the Atg5-Atg12-Atg16 complex, and LC3-I and Atg12 are activated by Atg7 during these process.[5,8,9] On the other hand, ER stress regulates eIF2α phosphorylation via activation of protein kinase regulated by RNA (PKR)-like ER kinase (PERK).[24] We examined whether polyQ72 induces the upregulation of *Atg5*, *Atg7*, *Atg12*, and *Atg16* mRNAs via eIF2α phosphorylation. In contrast with *Atg5*, *Atg7*, and *Atg16* mRNAs, *Atg12* as well as *CHOP* mRNA was upregulated by polyQ72 and their upregulation was inhibited by eIF2αA/A mutation, a knock-in to replace a phosphorylatable Ser^{51} with Ala^{51} (Figure 4a).[25] Moreover, thapsgargin induced the upregulation of *Atg12* mRNA as well as *CHOP* mRNA and their upregulation was inhibited by eIF2αA/A mutation (see Supplemental Figure 1c). We examined the effect of dominant-negative (DN)-PERK and an eIF2αA/A mutation on polyQ72-induced LC3 conversion (Figure 4b and c). PolyQ72-induced LC3 conversion, C/EBP homologous protein (CHOP), and Atg12 upregulation were inhibited by DN-PERK (Figure 4b) and the eIF2αA/A mutation (Figure 4c). Furthermore, short interfering RNA (siRNA) of *Atg12* inhibited polyQ72-induced upregulation of LC3 conversion without inhibiting the eIF2α phosphorylation (Figure 4d). In contrast with polyQ-induced LC3 conversion, starvation- and Rap-induced LC3 conversion were inhibited by the eIF2αA/A mutation (see Supplemental Figure 2b and d), but not inhibited by DN-PERK (see Supplemental Figure 2a and c). Thus, polyQ72 induced the Atg 12-dependent conversion of LC3-I to -II via ER-stress-mediated PERK/eIF2α phosphorylation.

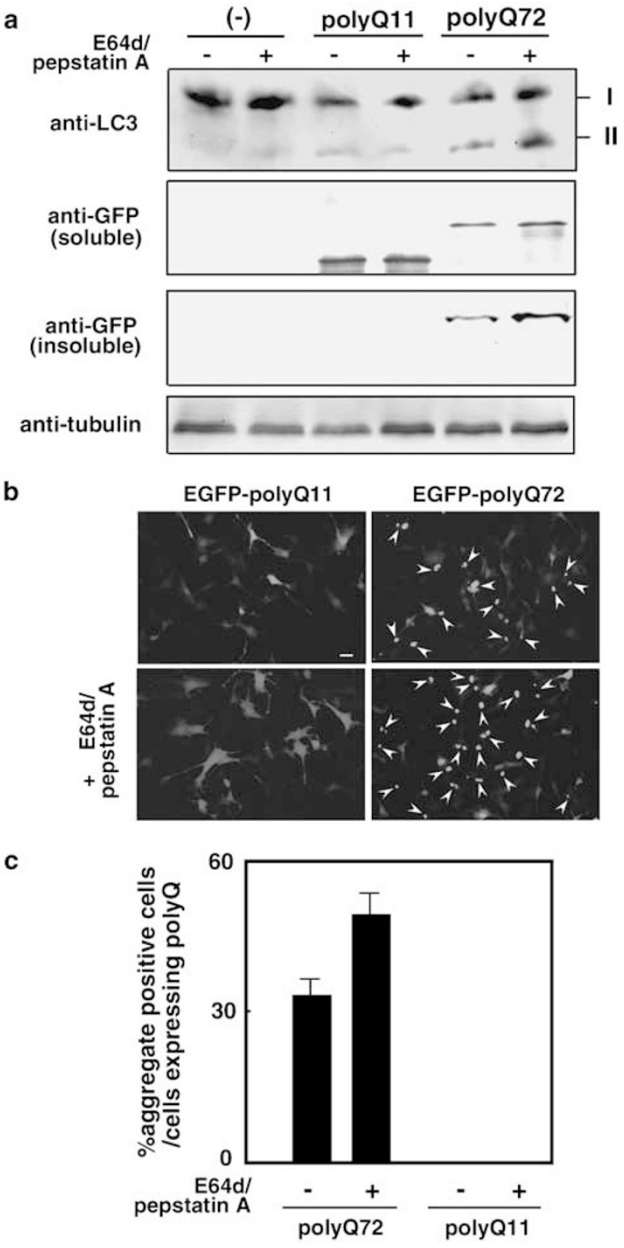

Figure 3 Effect of E64d and pepstatin A on the level of polyQ72 and polyQ72-induced LC3 conversion. (**a**) C2C5 cells were transfected with pEGFP-11CAG or pEGFP-72CAG and incubated in the presence or absence of E64d (10 μg/ml) and pepstatin A (10 μg/ml), then LC3 conversion and accumulation of polyQ were detected by immunoblot analysis. (**b**) Immunofluorescence images of polyQ11 or polyQ72 aggregation (green) in the presence or absence of E64d and pepstatin A. Arrows indicate EGFP-polyQ72 aggregates. Scale bar, 25 μm. (**c**) Effects of E64d and pepstatin A on polyQ11 and polyQ72 aggregation. Percentages of cells showing polyQ aggregates in cells expressing EGFP-polyQ11 or EGFP-polyQ72 were determined in the presence or absence of E64d and pepstatin A as described in Materials and Methods. Error bars represent S.E.M. of the percentage of cells with polyQ aggregates within cells expressing polyQ

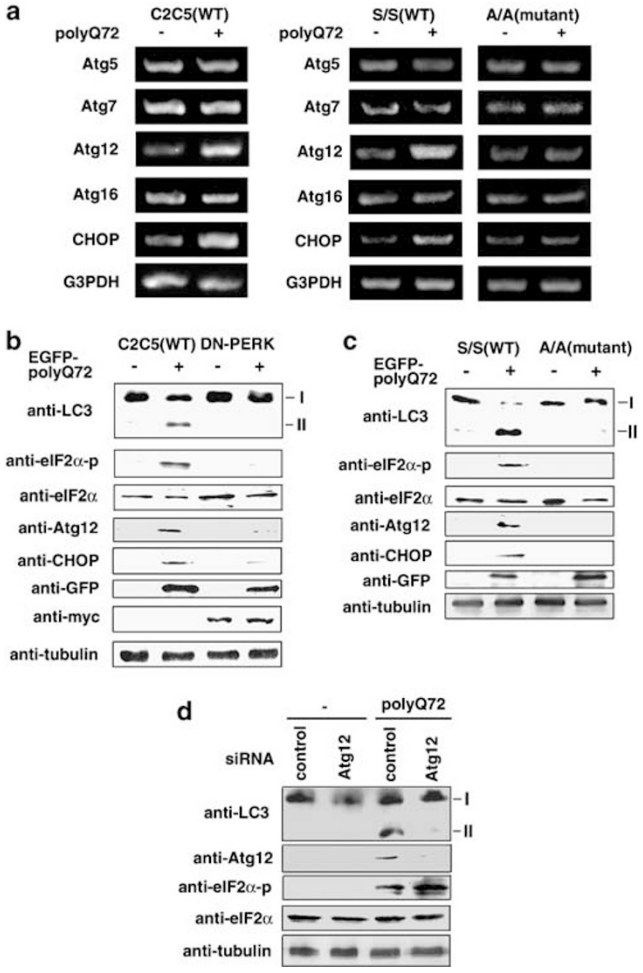

Figure 4 Involvement of PERK/eIF2α phosphorylation in polyQ72-induced LC3 conversion. (**a**) PolyQ72-induced upregulation of mRNA of *Atg5*, *7*, *12*, and *16* was examined by RT-PCR and involvement of eIF2α phosphorylation in the upregulation of *Atg* genes. C2C5 cells (left panels), eIF2αS/S and eIF2αA/A MEF cells (right panels) were transfected with pEGFP-72CAG and subjected to the RT-PCR analysis. (**b**–**c**) Effect of DN-PERK (**b**) and the eIF2α A/A mutation (**c**) on polyQ-induced LC3 conversion. C2C5 (WT) cells and DN-PERK cells (**b**) or eIF2αS/S (WT) and eIF2αA/A (mutant) MEF cells (**c**) were transfected with pEGFP-72CAG. LC3 conversion, eIF2α phosphorylation were detected by immunoblot analysis. (**d**) Inhibition of LC3 conversion by silencing of Atg12. C2C5 cells with silencing of control siRNA or Atg12 were transfected with pEGFP-72CAG, and LC3 conversion, eIF2α phosphorylation, expression of Atg 12 were detected by immunoblot analysis

Effect of eIF2α dephosphorylation and *Atg5* deficiency on polyQ aggregation and polyQ-induced caspase-12 activation. We examined involvement of eIF2α phosphorylation in polyQ72 aggregation and ER-stress-mediated cell death in cells showing polyQ72 aggregates. Caspase-12 was activated at ER of cells showing polyQ72 aggregates and then, activated caspase-12 became punctuated in apoptotic cells as shown previously (Figure 5a).[18,26] The eIF2α A/A mutation increased the population of the antiactivated caspase-12-positive cells in MEF cell expressing polyQ72 (3.4±1.1% of eIF2α S/S cells and 11.1±2.0% of eIF2α A/A cells) (Figure 5a, b) and also increased the number of cells showing polyQ72 aggregates (7.8±2.0% of eIF2α S/S cells and 30.4±3.5% of eIF2α A/A cells) (Figure 5a and c), and apoptotic feature (4.2±1.7% of eIF2α S/S cells and 11.5±0.9% of eIF2α A/A cells) (Figure 5d). Furthermore, the eIF2α A/A mutation increased the amount of insoluble polyQ72 and stimulated the polyQ72-induced caspase-12 activation (Figure 5f). Thus, in addition to polyQ72-induced caspase-12 activation, eIF2α phosphorylation inhibited the polyQ72 aggregation. However, the population of cells with caspase-12 activation was almost the same, about 30%, in eIF2αS/S and eIF2αA/A MEF cells showing polyQ72 aggregates; caspase-12 was activated in 31.6±3.3% of eIF2α S/S cells and 35.3± 2.5% of eIF2α A/A cells showing polyQ72 aggregates (Figure 5e).

We examined whether Atg5–Atg12–Atg16 complex-dependent LC3 conversion inhibits polyQ72 aggregate-induced caspase-12 activation (Figure 6). *Atg5* deficiency increased the accumulation of the insoluble form of polyQ72 (Figure 6a) and the number of cells showing polyQ72 aggregates (9.4±2.2% of Atg5+/+ cells and 38.6±3.2% of Atg5−/− cells) (Figure 6b). *Atg5* deficiency also increased the population of cells with caspase-12 activation (4.9±0.4% of Atg5+/+ cells and 10.9±0.7% of Atg5−/− cells) and apoptotic features (3.9±1.6% of Atg5+/+ cells and 11.6±0.9% of Atg5−/− cells) in cells expressing polyQ72 (Figure 6a, c and d), and increased the amount of insoluble polyQ72 and stimulated caspase-12 activation although it did not affect the amount of eIF2α phosphorylation and CHOP upregulation (Figure 6f). However, the population of cells with caspase-12 was almost the same, about 30%, in the Atg5+/+ cells and Atg5−/− cells showing polyQ72 aggregates; caspase-12 was activated in 32.9±2.1% of Atg5+/+ cells and 29.2±4.3% of Atg5−/− cells showing polyQ72 aggregates (Figure 6e).

Thus, Atg5–Atg12–Atg16 complex-dependent LC3 conversion inhibited ER-stress-mediated cell death with caspase-12 activation in cells expressing polyQ72. These results suggest that Atg5–Atg12–Atg16 complex-dependent LC3 conversion, leading to autophagy, inhibit polyQ72-induced ER-stress-mediated cell death with caspase-12 activation by degrading cytoplasmic polyQ72 aggregates (Figure 7).

Discussion

Biological significance of the autophagy formation in cells expressing cytoplasmic polyQ aggregates. In the present study, we showed that Atg5–Atg12–Atg16 complex-dependent LC3 conversion, a key factor for autophagy formation, inhibited the polyQ72-induced ER-stress-mediated cell death (Figures 2, 6). These results suggest that Atg5–Atg12-Atg16 complex-dependent LC3 conversion targets cytoplasmic aggregates of polyQ72. The cytoplasmic polyQ aggregates inhibit retrotranslocation of proteins from the ER and degradation of ER proteins in the ERAD system, resulting in the accumulation of malfolded proteins in the ER,[19] and induce ER-stress-mediated cell death.[18] Cytoplasmic aggregation of polyQ72 induces the accumulation of dysferlin, a protein involving in the Ca^{2+}-dependent membrane fusion process,[27] in the ER, resulting in the ER stress cell death (Fujita *et al.*, submitted elsewhere). Thus, it is likely that autophagy may inhibit the ER-stress-mediated

cell death by degrading protein aggregates, including polyQ72 aggregates, which cannot be degraded by the ubiquitine/proteasome system (Figure 7). However, when the protein aggregates are not degraded enough, continuous ER stress may produce excess autophagy, which unselectively degrades not only malfolded protein aggregates but also intracellular contents and induces severe neurodegeneration during excessive autophagic cell death. Autophagy may be protective in initial stages of polyQ-induced ER stress,[12] but may be deleterious in later stages.[2]

Degradation of malfolded protein aggregates by autophagy. Cytoplasmic polyQ aggregates can be degraded.[28] As large aggregates become difficult for proteasomes to degrade, involvement of other degradation systems such as autophagy have been suggested to degrade polyQ aggregates. Rap-promoted autophagy prevents polyQ-induced cell death by selectively degrading polyQ aggregates (Figure 1).[12,29] These data and our data showing colocalization of LC3 staining with polyQ72 aggregates (Figure 2c) support the possibility that autophagy degrades polyQ aggregates.

However, it is not yet clear how autophagy recognizes malfolded protein aggregates. *Atg7*-deficient mice show accumulation of ubiquitinated proteins in the liver,[10] strongly suggesting that autophagy as well as the ubiquitin/proteasome system is involved in the degradation of ubiquitinated proteins. PolyQ aggregates show antiubiquitin immunoreactivity[30] and that *Atg5* deficiency stimulates the accumulation of polyQ72 aggregates. Autophagy may preferentially degrade aggregates of ubiquitinated proteins rather than soluble nonubiquitinated proteins. The ubiquitination state and size of the protein aggregate may be a possible determinant for selective protein degradation by autophagy.

Involvement of eIF2α phosphorylation in LC3 conversion. Thus, LC3 conversion leading to autophagy is a cellular defense mechanism against polyQ72-induced ER-stress-mediated cell death. We examined the polyQ72-induced ER stress response signal stimulating LC3 conversion. ER stress stimulators, including Thap as well as polyQ72, induced LC3 conversion (see Supplemental Figure 1) and eIF2α phosphorylation. The polyQ72-induced LC3 conversion was inhibited in cells containing the eIF2α A/A mutation and DN-PERK (Figure 4b and c), strongly suggesting that the PERK/eIF2α pathway, an ER stress

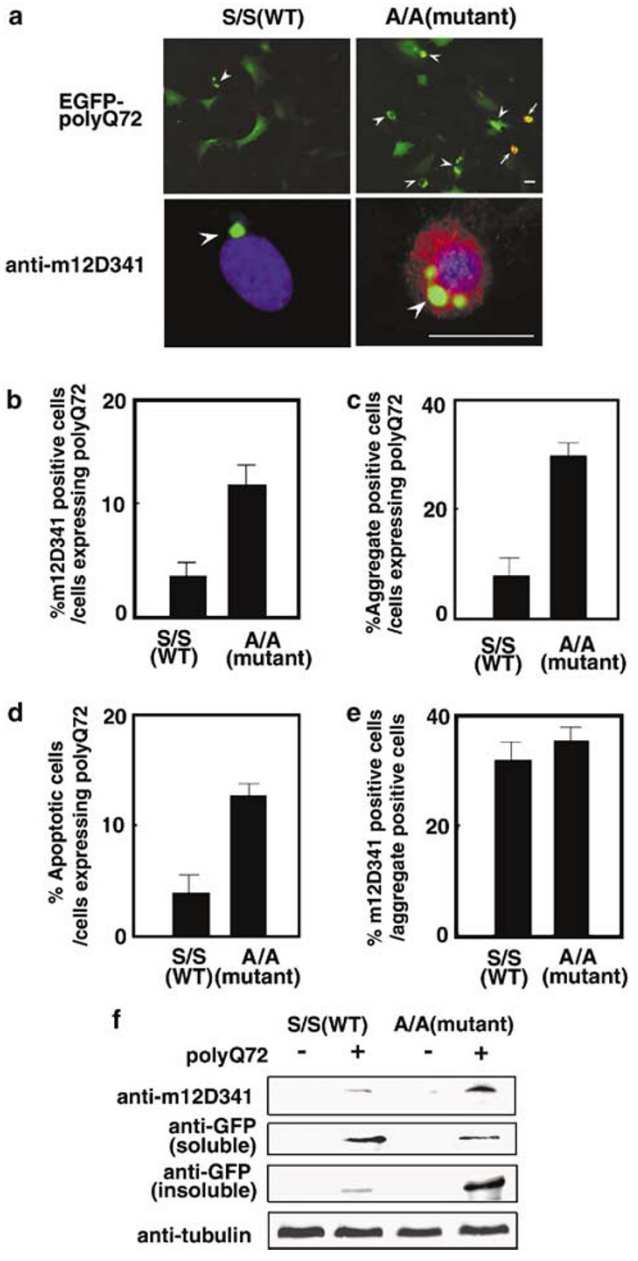

Figure 5 Involvement of eIF2α phosphorylation in polyQ72 aggregation and polyQ72-induced caspase-12 activation. (**a**) The effects of eIF2α dephosphorylation on polyQ72 aggregation and polyQ72-induced caspase-12 activation. eIF2αS/S (WT) MEF cells and eIF2αA/A (mutant) MEF cells were transfected with pEGFP-72CAG (EGFP-labeled: green), and immunofluorescence images of polyQ72 aggregation (green) and caspase-12 activation (red) (upper panels) were captured. Arrowheads indicate EGFP-polyQ72 aggregates and arrows indicate the cells colocalizing caspase-12 activation and EGFP-polyQ72 aggregates. Caspase-12 activation (lower panels) was detected by immunostaining using anti-m12D341 (rhodamine: red; Hoechst 33342: blue). Arrowheads indicate EGFP-polyQ72 aggregates. eIF2αA/A(mutant) MEF cells showed the apoptoti feautures with cell shrinkage and caspase-12 activation, but eIF2αS/S (WT) MEF cells did not. Scale bars, 25 μm. (**b**) Percentages of cells showing caspase-12 activation in cells expressing EGFP-polyQ72. Error bars represent S.E.M. of the percentage of cells with caspase-12 activation within cells expressing polyQ72. (**c**) Percentages of cells showing polyQ aggregates in cells expressing EGFP-polyQ72. Error bars represent S.E.M. of the percentage of cells with polyQ aggregates within cells expressing polyQ72. (**d**) Percentages of cells showing apoptotic feature in cells expressing EGFP-polyQ72. Error bars represent S.E.M. of the percentage of cells showing apoptotic feature within cells expressing polyQ72. (**e**) Percentages of cells showing caspase-12 activation in cells expressing EGFP-polyQ72 aggregate. Error bars represent S.E.M. of the percentage of cells with caspase-12 activation within cells expressing polyQ72 aggregate. The percentages were determined by counting 100–200 cells expressing EGFP-polyQ72 at 48 h after transfection. The values are averages of the percentages of the number of cells obtained in three experiments. (**f**) The effects of eIF2α dephosphorylation on polyQ72 aggregate-induced caspase-12 activation. eIF2αS/S (WT) MEF cells and eIF2αA/A (mutant) MEF cells were transfected with pEGFP-72CAG, and the caspase-12 activation were examined by immunoblot analysis

response signal, plays an essential role in polyQ72-induced LC3 conversion.

The relationship between autophagy and eIF2α phosphorylation has been shown during starvation-induced autophagy in *Saccharomyces cerevisiae* and during starvation- and virus-induced autophagy in mammalian cells.[31] In yeast, starvation results in the accumulation of uncharged tRNAs to activate GCN2, the sole eIF2α kinase. In mammals, there are at least four eIF2α kinases including GCN2, PKR, PERK, and HRI, which are activated by amino acid starvation, viral infection, ER stress, and heme depletion, respectively.[32] Virus induces autophagy via activation of PKR. Thus, it is possible that various stress conditions, including ER stress, that activate eIF2α kinases may have an ability to induce autophagy in mammalian cells by stimulating LC3 conversion.

Recently, it has been postulated the possibility that inhibition of mTOR, a mammalian target of Rap, induces autophagy and reduces the toxicity of polyQ expansions.[13] Rap fails to induce eIF2α phosphorylation in yeast with GCN2 defective in tRNA binding.[33] In contrast with polyQ72-induced LC3 conversion, Rap- as well as starvation-induced LC3 conversion was not mediated by PERK/eIF2α pathway (see Supplemental Figure 2). Inhibition of mTOR-mediated eIF2α phosphorylation may be an alternative pathway by which polyQ aggregates induce autophagy. Rap inhibits the ER-stress-mediated cell death (unpublished observation) but stimulates the starvation-induced autophagic cell death.[34] Thus, eIF2α phosphorylation does not inhibit the all types of stress-induced cell death.

The possible molecular mechanism of eIF2α phosphorylation inducing LC3 conversion. The molecular mechanism, by which eIF2α phosphorylation regulates LC3 conversion is not yet clear. eIF2α phosphorylation blocks the binding of initiator Met-tRNA to the ribosome by inhibiting the turnover of eIF2B and represses translation of most mRNAs. However, ATF4 mRNA, a member of the cAMP response-element-binding (CREB) family, is selectively translated under these conditions because of its small upstream open-reading frame (uORF) within the 5′ untranslated

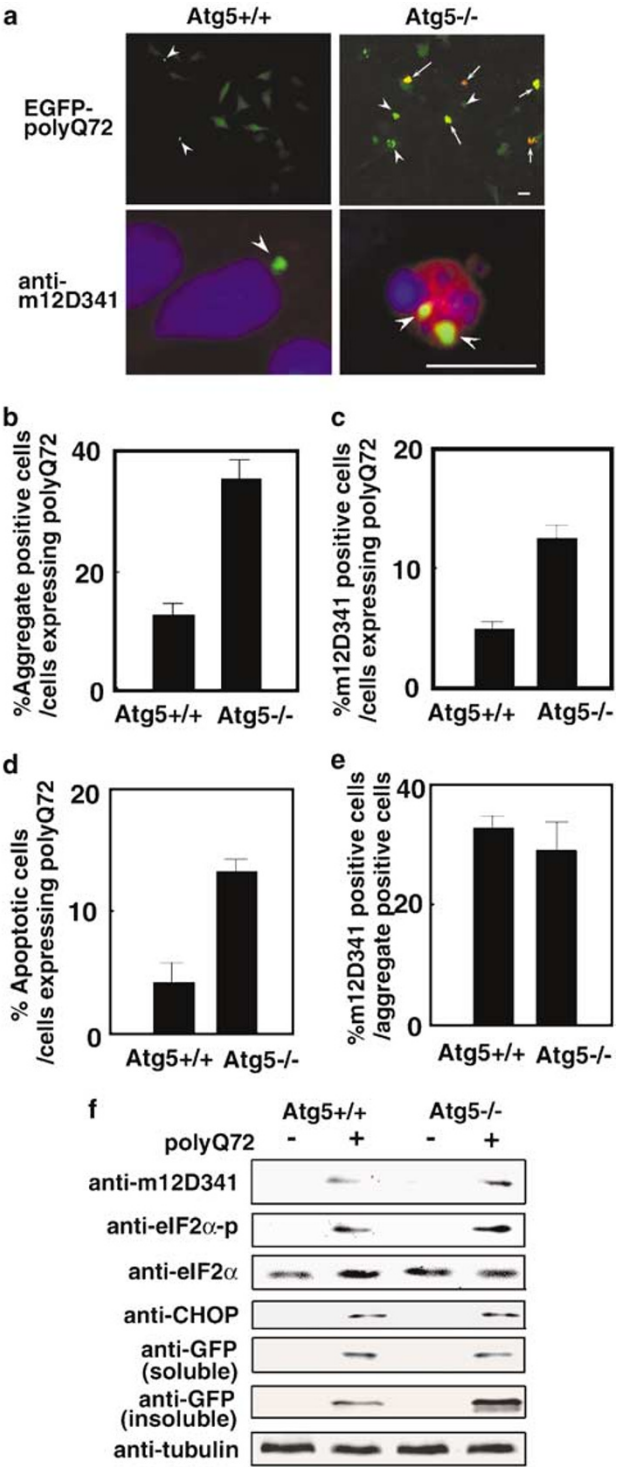

Figure 6 Effect of *Atg5*-deficiency on polyQ72 aggregation, and polyQ72- or Thap-induced caspase-12 activation. (**a**) Effect of *Atg5*-deficiency on polyQ72 aggregation and polyQ72-induced caspase-12 activation. Atg5 $+/+$ MEF cells and Atg5 $-/-$ MEF cells were transfected with pEGFP-72CAG (EGFP-labeled: green), and immunofluorescence images of polyQ72 aggregation (green) and caspase-12 activation (red) (upper panels) were captured. Arrowheads indicate EGFP-polyQ72 aggregates and arrows indicate the cells colocalizing caspase-12 activation and EGFP-polyQ72 aggregates. Caspase-12 activation (lower panels) was detected by immunostaining using anti-m12D341 (rhodamine: red; Hoechst 33342: blue). Arrowheads indicate EGFP-polyQ72 aggregates. Atg5 $-/-$ MEF cells showed the apoptotic features with cell shrinkage and caspase-12 activation, but Atg5 $+/+$ MEF cells did not. Scale bars, 25 μm. (**b**) Percentages of cells showing polyQ aggregates in cells expressing EGFP-polyQ72. Error bars represent S.E.M. of the percentage of cells with polyQ aggregates within cells expressing polyQ72. (**c**) Percentages of cells showing caspase-12 activation in cells expressing EGFP-polyQ72. Error bars represent S.E.M. of the percentage of cells with caspase-12 activation within cells expressing polyQ72. (**d**) Percentages of cells showing apoptotic feature in cells expressing EGFP-polyQ72. Error bars represent S.E.M. of the percentage of cells showing apoptotic feature within cells expressing polyQ72. (**e**) Percentages of cells showing caspase-12 activation in cells expressing EGFP-polyQ72 aggregate. Error bars represent S.E.M. of the percentage of cells with caspase-12 activation within cells expressing polyQ72 aggregate. The percentages were determined by counting 100–200 cells expressing EGFP-polyQ72 at 48 h after transfection. The values are averages of the percentages of the number of cells obtained in three experiments. (**f**) The effects of *Atg5*-deficiency on polyQ72 aggregate-induced caspase-12 activation. Atg5 $+/+$ MEF cells and Atg5 $-/-$ MEF cells were transfected with pEGFP-72CAG, and the caspase-12 activation and CHOP upregulation, eIF2α phosphorylation were examined by immunoblot analysis

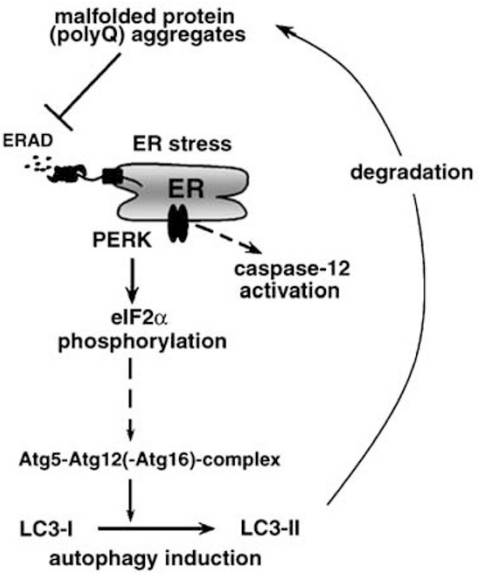

Figure 7 Involvement of eIF2α phosphorylation in malfolded protein polyQ72-induced LC3 conversion. PolyQ72 aggregates induce ER stress by inhibiting the retrotranslocation and/or ERAD activity.[19] The accumulation of malfolded proteins in the ER induces PERK/eIF2α phosphorylation, which induces LC3 conversion via upregulation of Atg12 and probably activation of Atg5–Atg12–Atg16 complex and stimulates autophagy degrading the polyQ72 aggregates. When LC3 conversion is not sufficient to reduce the polyQ72 aggregate, cells may undergo ER-stress-mediated cell death with caspase-12 activation[18]

region, called 'uORF bypath scanning system'.[35,36] ATF4 upregulates the transcription of downstream genes, including CHOP. *Atg12*, a component of Atg5–Atg12–Atg16 complex, as well as *CHOP* mRNA was selectively upregulated by polyQ72 via eIF2α phosphorylation (Figure 4a). Thus, one possible explanation is that the eIF2α phosphorylation-dependent selective translation of transcription factors may increase the upregulation of Atg12, resulting in the stimulation of the Atg5–Atg12–Atg16 complex formation followed by the promotion of the conversion of LC3-I to -II.

eIF2α phosphorylation-induced autophagy and inhibition of ER-stress-mediated cell death. Phosphorylation of eIF2α inhibits ER-stress-induced caspase-12 activation and ER-stress-mediated cells death.[37,38] Cells with phosphorylated eIF2α are resistant to oxidative stress[39] and inhibition of eIF2α dephosphorylation promotes survival of stressed cells.[40] *Atg5* deficiency did not inhibit Thap-induced caspase-12 activation (Supplemental Figure 3). Moreover, Rap inhibits the Thap-induced caspase-12 activation via eIF2α phosphorylation (unpublished observation), suggesting that eIF2α phosphorylation may inhibits Thap-induced cell death via preferentially inhibiting the caspase-12 activation. Thus, it may be possible that Rap inhibits the polyQ72-induced cell death by both pathways; stimulation of autophagy and inhibition of caspase-12 activation.

However, *Atg5* deficiency increased the population of cells with caspase-12 activation and apoptotic features in cells expressing polyQ72 although it did not affect the eIF2α phosphorylation and CHOP upregulation (Figure 6). eIF2α A/A mutation increased the number of cells showing polyQ72 aggregates, resulting in increase of the number of cells with caspase-12 activation (Figure 5), but did not increase the population of cells with caspase-12 activation in cells showing polyQ72 aggregates. These results suggest that eIF2α phosphorylation preferentially stimulates the LC3 conversion and the degradation of polyQ72 aggregates to inhibit the polyQ72 aggregates-induced cell death rather than the pathway inhibiting the caspase-12 activation.

Very recently, the accumulated mutant α_1-antitrypsin Z inhibitors in the ER has been shown to be degraded by autophagy.[41] We have also found that Atg5–Atg12-Atg16 complex-dependent LC3 conversion inhibits the accumulation of the mutated dysferlin in ER (Fujita *et al.*, submitted elsewhere). These results suggest the possibility that autophagye/lysosome as well as ubiquitine/proteasome is involved not only in the degradation of cytoplasmic protein aggregates such as polyQ aggregates but also in the degradation of the misfolded and unfolded ER protein in the ER as one of the ERAD degradation system to inhibit the ER-stress-mediated cell death. This possibility remains to be studied.

Recently, it has been shown that interaction between antiapoptotic protein Bcl-2 and the autophagy protein, Beclin-1, homolog of Atg6, represents a potentially important point of convergence of the apoptotic and autophagic machinery.[42–44] Dissociated Beclin-1 from Bcl-2 mediates the localization of other autophagy proteins to the preautophagosomal membrane and participates in autophagosome formation.[45,46] Thap increased the level of Beclin-1 protein and its dissociation from Bcl-2 (unpublished observation). ER-stress-induced dissociation of the Beclin-1 and Bcl-2 may also play a role in the regulation of the ER-stress-mediated apoptotic cell death and autophagic formation.

Conclusion

The scheme in Figure 7 shows the possible molecular mechanism of polyQ72- and ER-stress-induced LC3 conversion, LC3-I to -II, via activation of the PERK/eIF2α pathway. Atg5–Atg12–Atg16 complex-dependent LC3 conversion, which is stimulated by the activation of the PERK/eIF2α pathway in cells showing polyQ72 aggregates, is the cellular defense system that inhibits ER-stress-mediated cell death by degrading polyQ72 aggregates. Isolated membrane from the ER membrane may be elongated into an autophagosome by LC3-II activated by eIF2α phosphorylation.

Materials and Methods

Cell culture. C2C5 cells were P19 EC cells constitutively expressing *c-jun*.[47] MEFs from Atg5−/− and Atg5+/+ mouse embryos and C2C5 cells were cultured in α-minimum essential medium (α-MEM; Sigma, St Louis, MO, USA) supplemented with 10% fetal calf serum (FCS). MEFs from eIF2αS/S (WT) and eIF2αA/A (mutant) knock-in mouse embryos were cultured in DMEM (GIBCO, Grand Island, NY, USA) supplemented with 10% FCS, 0.1 mM nonessential amino acids solution (GIBCO), 1 × amino acids solution (GIBCO) and 100 U/ml penicillin/streptomycin (GIBCO) at 37°C in a humidified atmosphere of 5% CO_2.[25]

Plasmid construction and establishment of C2C5 cell lines. pEGFP-72CAG and pEGFP-11CAG were prepared as described previously.[48] Using restriction enzyme digestion and ligation, we subcloned the myc-tagged PERK(K618A) (DN-PERK)[24] into the pcDNA4/TO/myc-His expression

vector (Invitrogen, Carlsbad, CA, USA). pcDNA4/TO/myc-His-DN-PERK was transfected into C2C5 cells using the calcium phosphate method,[49] and clones expressing DN-PERK were selected by incubation with 50 μg/ml of zeocine and 25 μg/ml blastin (Invitrogen). Cells were cultured in α-MEM supplemented with 10% FCS with 5 μg/ml tetracycline at 37°C in a humidified atmosphere of 5% CO_2.

siRNA. siRNAs were designed and created at Nippon EGT Co. (Toyama, Japan). The sequences used were as follows: mouse *Atg 12* siRNA, 5′-CCUCGGAACAGUUGUUUAU-3′. Cells were transfected with 10 μg of siRNA using LipofectAMINE per the manufacturer's instructions. In the case of transfectio with complementary DNA and siRNA, DNA were transfected and after 12 h siRNAs were introduced.

Isolation of fragmented DNA. DNA isolation was performed according to the method of Prigent *et al*.[50]

Immunoblot analysis. ER stress signals were examined by immunoblot analysis using anti-m12D341, antisera against the cleavage site of mouse caspase-12 at D^{341},[26] anti-CHOP (Santa Cruz Biotechnology Inc., Santa Cruz, CA, USA), antitubulin (Sigma), anti-GFP (Boehringer Mannheim, Indianapolis, IN, USA), anti-eIF2α-p (antisera against phosphorylated serine at position 51 of eIF2α; Cell Signaling Technology, Beverly, MA, USA), anti-eIF2α (Cell Signaling Technology), and anti-myc (Santa Cruz Biotechnology Inc.), anti-Atg12 (ZYMED Laboratories, South San Francisco, CA, USA). LC3 conversion from I to II was examined by immunoblot analysis using anti-LC3.[20,23,51]

Cells were treated with Hank's Balanced Salt Solution (HBSS) or incubated with Bre (2 μg/ml), Tm (2 μg/ml), Thap (2 μM), Rap (10 μg/ml) (Sigma), and lysed with phosphate buffered saline (PBS) containing 1% Triton X-100. pEGFP-72CAG and pEGFP-11CAG (5 μg) were transfected using the calcium phosphate method. siRNA transfected cells were transfected with pEGFP-72CAG. Cells were incubated for the indicated period in the presence or absence of Rap (10 μg/ml), 3MA (10 mM), or E64d (10 μg/ml) (Calbiochem, La Jolla, CA, USA) and pepstatin A (10 μg/ml) (ICN Biochemicals Inc., Aurora, OH, USA) then lysed with PBS containing 1% Triton X-100.

After centrifugation at 10 000 $\times$ *g* for 10 min, the cell extracts (50 μg protein) were subjected to SDS polyacrylamide gel (12%) electrophoresis and immunoblot analysis as described previously.[18] Insoluble fraction were lysed into SDS sample buffer and subjected to SDS polyacrylamide gel (12%) electrophoresis. Quantification of the images was performed using NIH image (Dr. W Raeband National Institute of Health, Bethesda, MD, USA) programs.

Immunostaining. Cells were transfected with pEGFP-72CAG or pEGFP-11CAG and incubated in the presence or absence of Rap (10 μg/ml), or 3MA (10 mM). After the cells were fixed with 4% paraformaldehyde (PFA) in PBS at the indicated time, they were incubated with anti-LC3 or anti-m12D341 for 24 h at 4°C. They were then incubated with rhodamine-labeled goat anti-rabbit (Leinco Technologies Inc., St Louis, MO, USA) for 1 h at 37°C, and the nuclei were labeled with Hoechst 33342 (Molecular Probes, Eugene, OR, USA) and viewed with a confocal laser-scanning microscope (CSU-10, Yokogawa, Tokyo, Japan). Percentages of cells showing polyQ aggregates, caspase-12 activation, or apoptotic future were determined by counting 100–200 cells expressing EGFP-polyQ72 at 48 h after transfection in the presence or absence of Rap, 3MA, E64d and pepstatin A. The values are averages of the percentages of the number of cells obtained in three experiments.

12-week-old R6/2 transgenic mice[22] and B6CBAF1/J WT mice were obtained from Jackson lab. They were anesthetized with diethyl ether and perfused intracardially with 4% PFA in PBS. The brain was removed and incubated overnight in 4% PFA in PBS at 4°C and then soaked in 30% sucrose in PBS at 4°C overnight and embedded in optimal cutting temperature (OCT) compound (Sakura Finetec, Tokyo, Japan) before being frozen. Frozen sections of brain were cut on a cryostat and attached to slides coated with Vectabond reagent (Vector Laboratories, Burlingame, CA, USA) and double stained with antihuntingtin (EM48) (Chemicon International, Temecula, CA, USA) and with anti-eIF2α-p, anti-c-Jun-p (antisera against phosphorylated serine at position 63 of c-Jun; Cell Signaling Technology), anti-LC3 or anti-m12D341. Antihuntingtin reactivity was detected by the incubation with FITC-labeled goat anti-mouse immunoglobulin (Leinco Technologies Inc.) and anti-eIF2α-p, anti-c-Jun-p, anti-LC3 or anti-m12D341 reactivity was detected by he incubation with rhodamine-labeled goat anti-rabbit immunoglobulin for 1 h at 37°C to be viewed with a confocal laser scanning microscope. Cells showing punctuate vesicular anti-LC3 staining were counted as cells showing LC3 conversion.[21] Percentages of cells showing caspase-12 activation, c-Jun phosphorylation, eIF2α phosphorylation, and LC3 conversion were determined by counting 100–200 cells. The values are averages of the percentages of the number of cells obtained in three experiments.

RT-PCR. Complementary DNAs were synthesized from total RNA (1 μg) of cells treated with Thap (2 μM) or cells transfected with polyQ72 using reverse transcriptase (Stratagene, La Jolla, CA, USA). cDNAs were subjected to PCR as described in the manual from Perkin-Elmer (Branchburg, NJ, USA) using primers of mouse Atg5; forward primer, 5′-GGAAGAATGACAGATGAC-3′; and reverse primer, 5′-CTTTCAATCTGTTGGCTG-3′, Atg7; forward primer, 5′-ATGGGGGG ACCCTGGACTG-3′; and reverse primer, 5′-CAGAACAGTGTCGTCATC-3′, Atg12; forward primer, 5′-ATGTCGGAA GATTCAGAG-3′; and reverse primer, 5′-ATTT CTGGCTCATCCCCA-3′, Atg16; forward primer, 5′-GCGTTCGAGGAGATCATT-3′; and reverse primer, 5′-TTCCTT TGCTGCTTCTGC-3′, CHOP; forward primer, 5′-CAGAAGGAAGTGCATCTT CA-3′; and reverse primer, 5′-TACACTTCCGG AGAGACAGA-3′ and G3PDH (Toyobo, Osaka, Japan). The PCR fragments of the Atg genes were amplified as follows: 1 cycle at 95°C for 2 min, 25 cycles at 95°C for 1 min and 60°C for 1 min, and 1 cycle at 60°C for 7 min. The RT-PCR products were electrophoresed on 2% NuSieve agarose gels (FM Bioproducts, Rockland, ME, USA).

Acknowledgements. We thank Dr. David Ron (New York University School of Medicine) for kindly providing the myc-tagged PERK (K618A), and thank Dr. Noboru Mizushima (Tokyo Metropolitan Institute of Medical Science) for kindly providing the Atg5−/− MEF cells. This work was supported in part by Research Grants 14A-3 for Nervous and Mental Disorders, Research on Brain Science from the Ministry of Health and Welfare of Japan and the Human Science Foundation and NIH Grant DK42394 (RJK). E.F. and Y.K. are postdoctoral fellows of the JSPS Fellows.

1. Levine B. Eating oneself and uninvited guests: autophagy-related pathways in cellular defense. *Cell* 2005; **120**: 159–162.
2. Kegel KB, Kim M, Sapp E, McIntyre C, Castano JG, Aronin N *et al.* Huntingtin expression stimulates endosomal-lysosomal activity, endosome tubulation, and autophagy. *J Neurosci* 2000; **20**: 7268–7278.
3. Stefanis L, Larsen KE, Rideout HJ, Sulzer D, Greene LA. Expression of A53 T mutant but not wild-type alpha-synuclein in PC12 cells induces alterations of the ubiquitin-dependent degradation system, loss of dopamine release, and autophagic cell death. *J Neurosci* 2001; **21**: 9549–9560.
4. Ohsumi Y. Molecular dissection of autophagy: two ubiquitin-like systems. *Nat Rev Mol Cell Biol* 2001; **2**: 211–216.
5. Mizushima N, Ohsumi Y, Yoshimori T. Autophagosome formation in mammalian cells. *Cell Struct Funct* 2002; **27**: 421–429.
6. Kuma A, Hatano M, Matsui M, Yamamoto A, Nakaya H, Yoshimori T *et al.* The role of autophagy during the early neonatal starvation period. *Nature* 2004; **432**: 1032–1036.
7. Kabeya Y, Mizushima N, Ueno T, Yamamoto A, Kirisako T, Noda T *et al.* LC3, a mammalian homologue of yeast Apg8p, is localized in autophagosome membranes after processing. *EMBO J* 2000; **19**: 5720–5728.
8. Mizushima N, Yamamoto A, Hatano M, Kobayashi Y, Kabeya Y, Suzuki K *et al.* Dissection of autophagosome formation using Apg5-deficient mouse embryonic stem cells. *J Cell Biol* 2001; **152**: 657–668.
9. Klionsky DJ. The molecular machinery of autophagy: unanswered questions. *J Cell Sci* 2005; **118**: 7–18.
10. Komatsu M, Waguri S, Ueno T, Iwata J, Murata S, Tanida I *et al.* Impairment of starvation-induced and constitutive autophagy in Atg7-deficient mice. *J Cell Biol* 2005; **169**: 425–434.
11. Schmelzle T, Hall MN. TOR, a central controller of cell growth. *Cell* 2000; **103**: 253–262.
12. Ravikumar B, Duden R, Rubinsztein DC. Aggregate-prone proteins with polyglutamine and polyalanine expansions are degraded by autophagy. *Hum Mol Genet* 2002; **11**: 1107–1117.
13. Ravikumar B, Vacher C, Berger Z, Davies JE, Luo S, Oroz LG *et al.* Inhibition of mTOR induces autophagy and reduces toxicity of polyglutamine expansions in fly and mouse models of Huntington disease. *Nat Genet* 2004; **36**: 585–595.
14. Kopito RR, Ron D. Conformational disease. *Nat Cell Biol* 2000; **2**: E207–E209.
15. Sitia R, Braakman I. Quality control in the endoplasmic reticulum protein factory. *Nature* 2003; **426**: 891–894.
16. Nakagawa T, Zhu H, Morishima N, Li E, Xu J, Yankner BA *et al.* Caspase-12 mediates endoplasmic-reticulum-specific apoptosis and cytotoxicity by amyloid-beta. *Nature* 2000; **403**: 98–103.
17. Momoi T. Caspases involved in ER stress-mediated cell death. *J Chem Neuroanat* 2004; **28**: 101–105.

18. Kouroku Y, Fujita E, Jimbo A, Kikuchi T, Yamagata T, Momoi MY *et al.* Polyglutamine aggregates stimulate ER stress signals and caspase-12 activation. *Hum Mol Genet* 2002; **11**: 1505–1515.
19. Nishitoh H, Matsuzawa A, Tobiume K, Saegusa K, Takeda K, Inoue K *et al.* ASK1 is essential for endoplasmic reticulum stress-induced neuronal cell death triggered by expanded polyglutamine repeats. *Genes Dev* 2002; **16**: 1345–1355.
20. Jager S, Bucci C, Tanida I, Ueno T, Kominami E, Saftig P *et al.* Role for Rab7 in maturation of late autophagic vacuoles. *J Cell Sci* 2004; **117**: 4837–4848.
21. Mizushima N, Yamamoto A, Matsui M, Yoshimori T, Ohsumi Y. *In vivo* analysis of autophagy in response to nutrient starvation using transgenic mice expressing a fluorescent autophagosome marker. *Mol Biol Cell* 2004; **15**: 1101–1111.
22. Mangiarini L, Sathasivam K, Seller M, Cozens B, Harper A, Hetherington C *et al.* Exon 1 of the HD gene with an expanded CAG repeat is sufficient to cause a progressive neurological phenotype in transgenic mice. *Cell* 1997; **87**: 493–506.
23. Tanida I, Nubenatsy-Ikeguchi N, Uneno T, Kominami E. Lysosomal turnover, but not a cellular level, of endogenous LC3 is a marker for autophagy. *Autophagy* 2005; **1**: 84–91.
24. Harding HP, Zhang Y, Ron D. Protein translation and folding are coupled by an endoplasmic-reticulum-resident kinase. *Nature* 1999; **397**: 271–274.
25. Scheuner D, Song B, McEwen E, Liu C, Laybutt R, Gillespie P *et al.* Translational control is required for the unfolded protein response and *in vivo* glucose homeostasis. *Mol Cell* 2001; **7**: 1165–1176.
26. Fujita E, Kouroku Y, Jimbo A, Isoai A, Maruyama K, Momoi T. Caspase-12 processing and fragment translocation into nuclei of tunicamycin-treated cells. *Cell Death Differ* 2002; **9**: 1108–1114.
27. Bansal D, Campbell KP. Dysferlin and the plasma membrane repair in muscular dystrophy. *Trends Cell Biol* 2004; **14**: 206–213.
28. Yamamoto A, Lucas JJ, Hen R. Reversal of neuropathology and motor dysfunction in a conditional model of Huntington's disease. *Cell* 2000; **101**: 57–66.
29. Qin ZH, Wang Y, Kegel KB, Kazantsev A, Apostol BL, Thompson LM *et al.* Autophagy regulates the processing of amino terminal Huntingtin fragments. *Hum Mol Genet* 2003; **12**: 3231–3244.
30. Senut MC, Suhr ST, Kaspar B, Gage FH. Intraneuronal aggregate formation and cell death after viral expression of expanded polyglutamine tracts in the adult rat brain. *J Neurosci* 2000; **20**: 219–229.
31. Talloczy Z, Jiang W, Virgin HW, Leib DA, Scheuner D, Kaufman RJ *et al.* Regulation of starvation- and virus-induced autophagy by the eIF2alpha kinase signaling pathway. *Proc Natl Acad Sci USA* 2002; **99**: 190–195.
32. Dever TE. Gene-specific regulation by general translation factors. *Cell* 2002; **108**: 545–556.
33. Kubota H, Obata T, Ota K, Sasaki T, Ito T. Rapamycin-induced translational derepression of GCN4 mRNA involves a novel mechanism for activation of the eIF2 alpha kinase GCN2. *J Biol Chem* 2003; **278**: 20457–20460.
34. Uchiyama Y. Autophagic cell death and its execution by lysosomal cathepsins. *Arch Histol Cytol* 2001; **64**: 233–246.
35. Harding HP, Novoa I, Zhang Y, Zeng H, Wek R, Schapira M *et al.* Regulated translation initiation controls stress-induced gene expression in mammalian cells. *Mol Cell* 2000; **6**: 1099–1108.
36. Oyadomari S, Mori M. Roles of CHOP/GADD153 in endoplasmic reticulum stress. *Cell Death Differ* 2004; **11**: 381–389.
37. Harding HP, Zhang Y, Bertolotti A, Zeng H, Ron D. Perk is essential for translational regulation and cell survival during the unfolded protein response. *Mol Cell* 2000; **5**: 897–904.
38. Boyce M, Bryant KF, Jousse C, Long K, Harding HP, Scheuner D *et al.* A selective inhibitor of eIF2alpha dephosphorylation protects cells from ER stress. *Science* 2005; **307**: 935–939.
39. Tan S, Somia N, Maher P, Schubert D. Regulation of antioxidant metabolism by translation initiation factor 2alpha. *J Cell Biol* 2001; **152**: 997–1006.
40. Jousse C, Oyadomari S, Novoa I, Lu P, Zhang Y, Harding HP *et al.* Inhibition of a constitutive translation initiation factor 2alpha phosphatase, CReP, promotes survival of stressed cells. *J Cell Biol* 2003; **163**: 767–775.
41. Kamimoto T, Shoji S, Hidvegi T, Mizushima N, Umebayashi K, Perlmutter DH *et al.* Intracellular inclusions containing mutant alpha1-antitrypsin Z are propagated in the absence of autophagic activity. *J Biol Chem* 2006; **281**: 4467–4476.
42. Yu L, Alva A, Su H, Freundt PDE, Welsh S, Baehrecke EH *et al.* Regulation of an ATG7-beclin 1 program of autophagic cell death by caspase-8. *Science* 2004; **304**: 1500–1502.
43. Shimizu S, Kanaseki T, Mizushima N, Mizuta T, Arakawa-Kobayashi S, Thompson CB *et al.* Role of Bcl-2 family proteins in a non-apoptotic programmed cell death dependent on autophagy genes. *Nat Cell Biol* 2004; **6**: 1221–1228.
44. Pattingre S, Tassa A, Qu X, Garuti R, Liang H, Schneider MD *et al.* Bcl-2 antiapoptotic proteins inhibit Beclin 1-dependent autophagy. *Cell* 2005; **122**: 927–939.
45. Liang XH, Kleeman LK, Jiang HH, Gordon G, Goldman JE, Berry G *et al.* Protection against fatal Sindbis virus encephalitis by beclin, a novel Bcl-2-interacting protein. *J Virol* 1998; **72**: 8586–8596.
46. Kihara A, Kabeya Y, Ohsumi Y, Yoshimori T. Beclin-phosphatidylinositol 3-kinase complex functions at the trans-Golgi network. *EMBO Rep* 2001; **2**: 330–335.
47. Odaka A, Tsukahara T, Momoi M, Momoi T. c-jun inhibited the alternative splicing of neuron-specific amyloid precursor protein, but stimulated the non-neuron type one in P19 EC cells. *Biochem Biophys Res Commun* 1995; **206**: 821–828.
48. Kouroku Y, Fujita E, Urase K, Tsuru T, Setsuie R, Kikuchi T *et al.* Caspases that are activated during generation of nuclear polyglutamine aggregates are necessary for DNA fragmentation but not sufficient for cell death. *J Neurosci Res* 2000; **62**: 547–556.
49. Graham FL, Van der Eb AJ. A new technique for the assay of infectivity of human adenovirus 5 DNA. *Virology* 1973; **52**: 456–467.
50. Prigent P, Blanpied C, Aten J, Hirsch F. A safe and rapid method for analyzing apoptosis-induced fragmentation of DNA extracted from tissues or cultured cells. *J Immunol Methods* 1993; **160**: 139–140.
51. Nemoto T, Tanida I, Tanida-Miyake E, Minematsu-Ikeguchi N, Yokota M, Ohsumi M *et al.* The mouse APG10 homologue, an E2-like enzyme for Apg12p conjugation, facilitates MAP-LC3 modification. *J Biol Chem* 2003; **278**: 39517–39526.

Supplementary Information accompanies the paper on Cell Death and Differentiation website (http://www.nature.com/cdd)